SOLUTION OF LAPLACE'S EQUATION FOR A RIGID CONDUCTING CONE AND PLANAR COUNTER-ELECTRODE: COMPARISON WITH THE SOLUTION TO THE TAYLOR CONICAL MODEL OF A FIELD EMISSION LMIS

M. Chung, P. Cutler, T. Feuchtwang, N. Miskovsky

SOLUTION OF LAPLACE'S EQUATION FOR A RIGID CONDUCTING CONE AND PLANAR COUNTER-ELECTRODE: COMPARISON WITH THE SOLUTION TO THE TAYLOR CONICAL MODEL OF A FIELD EMISSION LMIS+

M. Chung, P.H. Cutler, T.E. Feuchtwang and N.M. Miskovsky++

Department of Physics, The Pennsylvania State University, University Park, Pennsylvania 16802, U.S.A.

Résumé - Bien que le problème électrostatique d'un cône conducteur rigide et d'une contre-électrode plane n'ait jamais été résolu exactement, nous montrons, en accordant les solutions à courte et à grande distance, que le champ au voisinage de l'apex est donné approximativement par :

$$V(R,\theta) \approx V_0 \left[1 - 0.92062 \left(\frac{R}{R_0}\right)^{0.5} P_{1/2}(\cos\theta) - 0.0742 \left(\frac{R}{R_0}\right)^{1.9} P_{1.9}(\cos\theta) - 0.00342 \left(\frac{R}{R_0}\right)^{3.3} P_{3.3}(\cos\theta) \right]$$

Il est aussi démontré que la solution de Taylor au problème électrostatique d'un cône rigide et d'une contre-électrode plane ne satisfait pas l'équation de Laplace pour les configurations réelles d'électrodes utilisées dans les sources d'ions à métal liquide et dans d'autres expériences sur des fluides conducteurs soumis à des champs électrostatiques.

Abstract - Although the electrostatic problem of a rigid conducting cone and infinite planar counter-electrode has never been solved exactly, we show, by matching the near and far solutions, that the field in the vicinity of the apex is approximately given by

$$V(R,\theta) \approx V_0 \left[1 - 0.92062 \left(\frac{R}{R_0}\right)^{0.5} P_{1/2}(\cos\theta) - 0.0742 \left(\frac{R}{R_0}\right)^{1.9} P_{1.9}(\cos\theta) - 0.00342 \left(\frac{R}{R_0}\right)^{3.3} P_{3.3}(\cos\theta) \right]$$

It is also explicitly demonstrated that Taylor's solution to the electrostatic problem of a rigid cone and non-planar counter-electrode model does not satisfy the Laplace Equation for the actual electrode configurations used in field emission liquid metal ion sources and other experiments on electrostatically stressed conducting fluids.

I. INTRODUCTION

In this paper we present a solution of the electrostatic problem of a conducting cone and infinite planar counter-electrode. Although this conical configuration was assumed by Taylor /1/ and others /2,3/ to be the equilibrium shape of a conducting fluid in an electric field prior to and at onset of instability, the difficulty in solving Laplace's equation for the exact geometry and other constraints /4/, prompted Taylor to choose a different model for the counter-electrode. Using the conical shape for the electrostatically stressed fluid, Taylor invoked dimensionality arguments to show that the only field distribution consistent with a cone that satisfied his form of the Laplace condition is given by

$$V(R,\theta) = V_0 + A\, R^{1/2}\, P_{1/2}(\cos\theta) \quad , \tag{1}$$

where notation is defined in Ref. 1. It then follows that the counter-electrode necessary to produce this field is

$$R = R_0[P_{1/2}(\cos\theta)]^{-2} \quad . \tag{2}$$

The non-planar nature of this electrode is clearly illustrated in Figure 1a which is a reproduction of Taylor's apparatus /1/ designed to "produce" the conical field given by Eq. (1). Figure 1b is a schematic of these electrodes; notation for the analysis to be described is given in the figure. Also illustrated is Taylor's proposed conical shape of the conducting fluid surface just prior to the onset of instability. It is important to note that in the experimental procedure used by Taylor, he filled the top of the truncated cone, denoted by C, with precisely the volume of fluid necessary to complete the apex of the cone. This was done to ensure that there would be exactly the conical shape to satisfy Eqs. (1) and (2).

We now demonstrate that Taylor's solution to the electrostatic problem of a rigid cone and idealized counter-electrode does not satisfy the Laplace equation for the actual experimental configurations for field emission liquid metal ion sources /5/ and other experiments on electrostatically stressed conducting fluids /6/. The geometry common to these experiments consists of essentially an infinite planar-counter-electrode centered above the source. This is illustrated schematically in Fig. 2a, the corresponding idealization as a rigid cone is shown in Fig. 2b. A qualitative plot of the potential distribution is also depicted in Fig. 2b. Although Taylor's solution, given by Eq. (1) (hereafter denoted by $V^T(R,\theta) \equiv V^T$) satisfies the Dirichlet boundary condition $V = 0$, on the idealized counter-electrode, the potential V^T never satisfies this boundary condition on a planar counter-electrode. Since the constant A in Eq. (1) is easily shown to be $-V_0/R_0^{1/2}$, it follows from the application of the boundary condition on the planar electrode that $V^T = V_0\,[1 - P_{1/2}(\cos\theta)\sec^{1/2}\theta]$ should be equal to zero for all θ. However the bracket term cannot be zero since

$$P_{1/2}(\cos\theta) = \frac{2}{\pi}\,[2E(\sin\tfrac{1}{2}\theta) - K(\sin\tfrac{1}{2}\theta)] \tag{3}$$

is never equal to $\sec^{-1/2}\theta$ for any value of θ. In Eq. (3) E and K are the elliptic integrals of the 1st and 2nd kind respectively /7/.

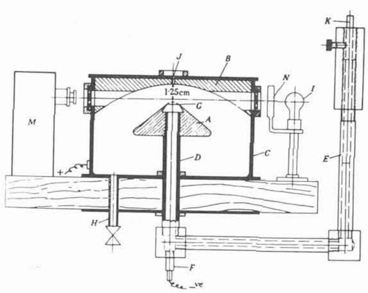

a

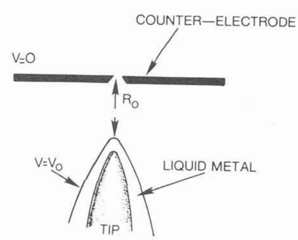

a

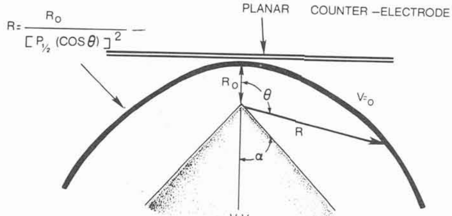

b

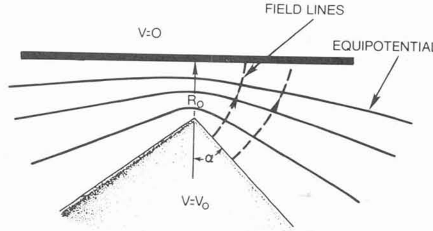

b

Fig. 1a. Diagram of Taylor's experimental apparatus /1/. The surface A is the truncated cone of half-angle 49.3°; the counter-electrode is the metal surface B.

1b. Schematic comparison of the Taylor electrode configuration and the planar counter-electrode model.

Fig. 2a. Schematic of the electrode configuration in a typical LMIS.

2b. The cone and planar electrode model of an LMIS.

II. SOLUTION OF LAPLACE'S EQUATION FOR THE CONE AND INFINITE PLANE

In this section we present a solution for the electrostatic problem of an infinite cone and planar counter-electrode and show that the resulting fields near the apex differ significantly, qualitatively and quantitatively, from Taylor's solution given by Eq. (1).

Consider first the general solution of Laplace's equation in spherical coordinates and with azimuthal symmetry,

$$\nabla^2 V = \frac{1}{R^2}\frac{\partial}{\partial R}\left(R^2 \frac{\partial V}{\partial R}\right) + \frac{1}{R^2 \sin\theta}\frac{\partial}{\partial \theta}\left(\sin\theta \frac{\partial V}{\partial \theta}\right) = 0 \quad , \tag{4}$$

subject to the boundary conditions $V = 0$ on the counter-electrode and $V = V_0$ on the cone. The model and coordinates are defined in Fig. 3. The general solution is

$$V(R,\theta) = \sum_{\nu} (A_\nu R_\nu + B_\nu R^{-\nu-1}) P_\nu(\cos\theta) \tag{5}$$

with $\mathrm{Re}\,\nu \geq -\frac{1}{2}$ /8/.

Since the electrodes do not correspond to any of the coordinate surfaces in the known separable coordinate systems, there is no closed form solution for the potential $V(R,\theta)$. However, the spherical coordinate system was selected in this problem because the coordinate surface $\theta = \theta_0$ corresponds to the surface of the cone.

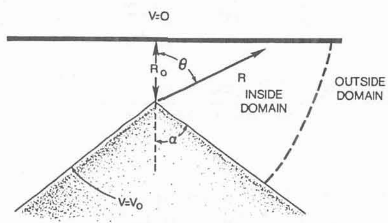

Fig. 3. Schematic diagram defining the notation and domains in the solution of Eq. (4).

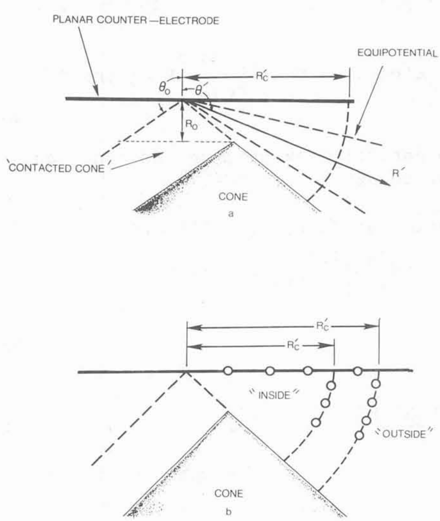

Fig. 4a. A schematic illustration of the "contacted" cone model.
4b. A schematic diagram illustrating the boundary matching procedure.

To approximate the solution we use the following procedure:

1. Solve Laplace's equation exactly in the inside domain or the near region of the apex of the cone (see Fig. 3).
2. Approximate the solution in the outside domain with the exact solution of the "contacted" cone problem, which is described below.
3. Match the two solutions on the boundary surface between the two regions to determine the expansion coefficients for the solution in the inside domain.

In the inside or near region, where the infinite series in inverse powers of R must vanish, the exact solution is

$$V(R,\theta) = V_0 + \sum_{\nu_s} A_{\nu_s} R^{\nu_s} P_{\nu_s}(\cos\theta) \quad (R < R_c') \ , \tag{6}$$

where R_c', which denotes the "boundary surface," is defined in Fig. 4a. The ν_s's are solutions of the equation

$$P_{\nu_s}(\cos\theta_0) = 0 \quad \text{for} \quad \theta_0 = \pi - \alpha \quad , \tag{7}$$

and define the zeros of the Legendre functions, P_{ν_s}'s, of non-integral index /9/.

This condition on the ν_s's ensures that the boundary condition $V = V_0$ is satisfied on the cone. In the outside or far regions, that is $R > R_c'$, the solution $V(R,\theta)$ is approximated by the exact potential for a "contacted" cone, which is schematically shown in Figure 4b. As seen in the figure, the contacted cone is obtained by displacing the actual cone an upward distance R_0 sec along the edge of the cone. It is assumed that the two "contacted" electrodes are separated by an infinitesimally thin insulating layer. The resulting configuration of electrodes in just a special case of the biconical antenna /10/ where the upper "cone" has been folded out with a half-angle of $\pi/2$.

The exact solution to this problem, which is independent of R, is given by

$$V'(R',\theta') = V'(\theta') = V_0\left[\ln(\tan\frac{\theta'}{2})\Big/\ln(\tan\frac{\theta_0}{2})\right], \tag{8}$$

with prime denoting the "contacted" cone coordinates and other symbols are defined in Fig. 4a. It is evident that for $R' \gg R_0$, this solution is a good approximation for the separated cone problem. Therefore, using the following relations between the coordinates for the contacted and separated cones

$$\tan\frac{\theta'}{2} = \frac{R' - R\cos\theta + R_0}{R\sin\theta + R_0\tan\alpha} \tag{9a}$$

and

$$R' = [R^2 + R_0^2\sec^2\alpha - 2RR_0\sec\alpha\cos(\theta+\alpha)]^{1.2}, \tag{9b}$$

we obtain

$$V'(\theta') \approx V(R,\theta) = V_0\ln\left[\frac{[R^2+R_0^2\sec^2\alpha-2RR_0\sec\alpha\cos(\theta+\alpha)]^{1/2} - R\cos\theta + R_0}{R\sin\theta + R_0\tan\alpha}\right]\Big/\ln\left(\tan\frac{\theta_0}{2}\right). \tag{10}$$

To find the expansion coefficients in the solution for the near region, we match Eqs. (6) and (10) on the "boundary surface" defined by $R' = R_c'$. The matching prodecure is done on different "boundaries" (i.e., different values of R_c') and with different numbers of sample points until the coefficients are stable to within 0.1%. This procedure is illustrated schematically, with sample points, in Fig. 4b. The resulting stable solution is

$$V(R,\theta) = V_0\left[1-0.9206\left(\frac{R}{R_0}\right)^{0.5}P_{0.5}-0.0742\left(\frac{R}{R_0}\right)^{1.9}P_{1.9}(\cos\theta)-0.0034\left(\frac{R}{R_0}\right)^{3.3}P_{3.3}(\cos\theta)\right]. \tag{11}$$

With this solution, the boundary conditions are satisfied exactly on the cone, and are stable to within 0.1% on the infinite planar counter-electrode.

The field components corresponding to the potential given by Eq. (11) are

$$E_R = -\frac{dV}{dR} = \frac{V_0}{R_0}\left[0.46029\left(\frac{R}{R_0}\right)^{-1/2}P_{0.5}(\cos\theta) + 0.14105\left(\frac{R}{R_0}\right)^{0.9}P_{1.9}(\cos\theta)\right.$$
$$\left. - 0.011319\left(\frac{R}{r_0}\right)^{2.3}P_{3.3}(\cos\theta)\right] \tag{12a}$$

$$E_\theta = -\frac{1}{R}\left(\frac{dV}{d\theta}\right) = -\left(\frac{V_0}{R_0}\right)\left[0.46029\,\frac{P_{-0.5}(\cos\theta)-\cos P_{0.5}(\cos\theta)}{\sin\theta}\left(\frac{R}{R_0}\right)^{-0.5}\right]. \tag{12b}$$

In order to compare with Taylor's results, we list below the corresponding fields for the potential, given by Eq. (1):

$$E_R^T = -\frac{dV}{dR} = 0.5\left(\frac{V_0}{R_0}\right)\left(\frac{R}{R_0}\right)^{-0.5}P_{0.5}(\cos\theta) \tag{13a}$$

$$E_\theta^T = -\frac{1}{R}\frac{dV}{d\theta} = -\;0.5\left(\frac{V_0}{R_0}\right)\left[\frac{P_{-0.5}(\cos\theta)-\cos P_{0.5}(\cos\theta)}{\sin\theta}\right]\left(\frac{R}{R_0}\right)^{-0.5}. \tag{13b}$$

III. COMPARISON OF THE FIELDS AND CRITICAL VOLTAGE

It is particularly important to note that although the first two terms of the solution for the planar counter-electrode model (Eq. (11)) have the same functional form as the Taylor solution for the curved counter-electrode (Eq. (1)), the coefficients of the second terms differ by about 10%. Furthermore the higher- order terms in Eq. (11) lead to a different R-dependence and make significant contributions especially along the axis of the cone. The resulting field dependence is not simply $R^{-1/2}$ and this leads to both qualitative and quantitative differences in the two field distributions. This is illustrated first in Figures 5a and b which are numerical plots of the potential and field distributions for a cone with the Taylor half-angle $\alpha = 49.3°$. These have been obtained using Eqs.(12) and (13) for the planar electrode and Taylor model respectively. Most significant is the more divergent behavior of the field lines near the apex of the cone in the Taylor model. Thus apart from the question of whether the conical model is even a correct description of an LMIS /4,10/ the use or application of the Taylor fields in the calculations of, say space charge or ion trajectories in an LMIS, will lead to results which are inconsistent with those obtained from the model with a planar counter-electrode.

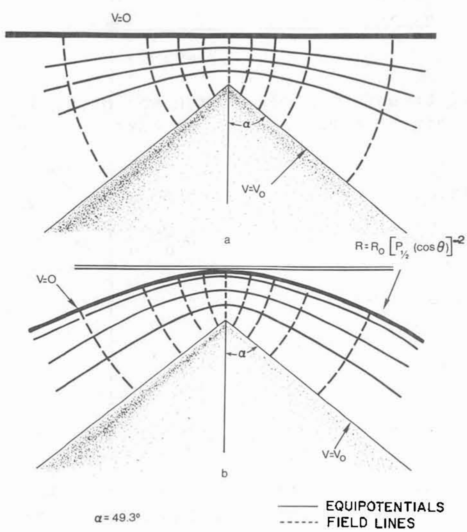

Fig. 5. Numerical plots of the potential and field distribution for
a. Taylor cone with planar counter-electrode and
b. Taylor cone and idealized non-planar counter-electrode given respectively by Eqs. (11) and (12) and Eqs. (1) and (13).

In Tables I and II we compare quantitively the fields, for the planar and Taylor models, along the exterior cone axis and the surface of the cone respectively. Distances are normalized in terms of the apex-extractor electrode distance R_0, and the fields expressed in units of (V_0/R_0). Along the direction of the axis the component E must, by symmetry, be zero, and only the radial components of the fields are compared. Similarly on the surface of the cone, defined by $\theta_0 = \pi - \alpha$, the radial component of the field is zero, so that only the θ-component is compared in Table II. In both cases the calculated fields differ from each other by about 10-25% over the range considered. These differences are further manifested in the calculation of the critical breakdown voltages, which can be experimentally determined.

Using the Taylor equilibrium condition /1/

$$\frac{\gamma \cot\alpha}{R} = \frac{1}{8\pi}\left(\frac{1}{R}\frac{dV}{d\theta}\right)^2 \tag{14}$$

and Eq. (1), in the form,

$$V = V_0\left[1 - \left(\frac{R}{R_0}\right)^{1/2} P_{1/2}(\cos\theta)\right], \tag{15}$$

the critical voltage for breakdown in the Taylor model, $V_0^{C,T}$, is given by

$$V_0^{C,T} = \frac{1}{0.97445}\sqrt{8\pi R_0 \gamma \cot\alpha}\ . \tag{16}$$

The corresponding expression for the planar electrode model, obtained using Eqs. (14) and (11) is

$$V_0^C = \frac{1}{0.89706}\,\frac{\sqrt{8\pi R_0 \gamma \cot\alpha}}{\left[1 - 0.12208\left(\frac{R}{R_0}\right)^{1/4} \cdots\right]} \tag{17}$$

Table I. Comparison of Fields on Axis

R/R_0	$E_R/(V_0/R_0)$	$E_R^T/(V_0/R_0)$	$(E_R-E_R^T)/E_R \times 100$
0.00001	145.556	158.114	8.6%
0.0001	46.029	50.000	8.6
0.001	14.566	15.811	8.6
0.01	4.605	5.000	8.6
0.10	1.473	1.581	7.3
1.00	0.621	0.500	19.5

Table II. Comparison of Fields on Surface of the Cone

R/R_0	$E_\theta/(V_0/R_0)$	$E_\theta^T/(V_0/R_0)$	$-(E_\theta-E_\theta^T)/E_\theta \times 100$
0.00001	283.675	308.148	8.6%
0.0001	89.706	97.445	8.6
0.001	28.367	30.815	8.6
0.01	8.969	9.745	8.7
0.10	2.823	3.081	9.1
1.00	0.786	0.974	24.0

We first use Eqs. (16) and (17) for the case of transformer oil, which was studied experimentally by Taylor /1/. The results are given in Table III. We note that in

Table III. Comparison of the Critical Voltages for Breakdown

R/R_0	V_0^C(volts)	$V_0^{C,T}$(volts)	$(V_0^C-V_0^{C,T})/V_0^C\times100$
0.00001	7.129×10^3	6.5×10^3	9.4%
0.0001	7.129	"	9.4
0.001	7.129	"	9.4
0.010	7.130	"	9.4
0.10	7.164	"	9.5
1.00	8.120	"	20.0

Taylor's model, the critical voltage is constant over the surface of the cone. By contrast, our calculated potential distribution predicts a position dependent breakdown voltage, which is in agreement with the local nature of the observed instabilities in both LMIS /12/ and other experiments on electrostatically stressed fluids /6/ including Taylor's own observations /1/. Although we obtain remarkably good agreement with Taylor's experimental value of $V_0^{C,exp} = 7.2\text{-}7.6 \times 10^3$ volts, the agreement is probably more fortuitous than real. We have also calculated the critical voltages for liquid gold and gallium in the two models and again find differences of about 10-25% along the surface of the cone. However, both sets of the calculated values are about 2-3 times the experimental values /3,13/. This may be attributable to the fact that actual shape of the liquid metal source is not conical but probably cuspidal or cuspidal-like /12/, leading to higher fields and consequently lower breakdown voltages near the apex. Calculations of the critical breakdown voltages for the cuspidal model of an LMIS are now in progress. It is important to stress that the Taylor cone model and his resultant condition for equilibrium (see Eq. (14)] predicts a constant value of the critical voltage over the entire surface of the cone, i.e., global. This is in disagreement with experimental observations discussed earlier as well as a recent theoretical analysis of the stability of electrostatically stressed conducting fluids /14/ which clearly demonstrates that the onset of instability (i.e., breakdown) is a local phenomenon.

In conclusion, the significance of the electrostatic solution we have obtained for the conducting cone with an infinite planar counter-electrode can be summarized as follows:

1. It is never equivalent to Taylor's solution for the idealized non-planar electrode geometry.
2. The field dependence, in contrast to Taylor's model, is not simply $R^{-1/2}$ and consequently is incompatible with the Taylor stress condition for equilibrium.

Acknowledgements

The authors wish to express their thanks to Professor E. Kazes for helpful conversations.

REFERENCES

+This work was supported in part by the Division of Materials Research, National Science Foundation, Grant No. DMR-8108829.

++Department of Physics, The Pennsylvania State University, Altoona Campus, Altoona, Pennsylvania 16803.

1. G. Taylor, "Disintegration of Water Droplets in an Electric Field," Proc. Roy. Soc. London 280A, 383 (1964).

2. R. Clamplitt, Advances in Molten Metal Field Ion Sources," Nuclear Instruments and Methods 189, 111 (1981).

3. R. Gomer, "On the Mechanism of Liquid Metal Electron and Ion Sources," Appl. Phys. 19, 365 (1979).

4. M. Chung, P. H. Cutler, T. E. Feuchtwang, N. M. Miskovsky and N. Sujatha, "On the Theory of the Equilibrium Configuration and Stability of an Electrostatically Stressed Fluid: Application to Liquid Metal Ion Sources," to be published in Scanning Electron Microscopy 1984.

5. See, for example,
a) C. A. Evans, Jr. and C. D. Hendricks, "An Electrohydrodynamic Ion Source for Mass Spectrometry of Liquids," Rev. Sci. Inst. 43, 1527 (1972).
b) F. W. Martin, "On the Feasibility of Microscopy with High Energy Heavy Ions," Annals of the New York Academy of Science, Vol. 306, p. 262 (1978).
c) G. L. Mair and A. von Engel, "Mass Transport in Liquid Gallium Ion Beam Sources," J. Phys. D: Appl. Phys. 14, 1721 (1981).
d) T. Venkatesan, A. Wagner, G. L. Mash and D. Barr, "Giant Stark Broadening of Atomic Gallium Emission Near a High Field Tip," Appl. Phys. Letters 39, 9 (1981).

6. a) J. Zeleny, "On the Condition of Instability of Electrified Drops with Application to the Electrical Discharge from Liquid Points," Proc. Camb. Phil. Soc. 18, 71 (1915).
b) C. T. R. Wilson and G. I. Taylor, "The Bursting of Soap Bubbles in a Uniform Electric Field," Proc. Camb. Phil. Soc. 22, 728 (1925).
c) W. A. Mackey, "Some Investigations on the Deformation and Breaking of Water Droplets in Strong Electric Fields," Proc. Rey. Soc. A133, 565 (1931).

7. M. C. Gray, "Legendre Functions of Fractional Order," Quarterly of Appl. Math. 11, 311 (1953).

8. J. P. Jackson, Classical Electrodynamics, 2nd edition (J. Wiley and Sons, Inc., New York, 1975).

9. R. N. Hall, "Application of Non-Integral Legendre Functions to Potential Problems," J. Appl. Phys. 20, 925 (1949).

10. J. A. Schelkunoff, Advanced Antenna Theory, (J. Wiley and Sons, New York, 1956).

11. N. Sujatha, P. H. Cutler E. Kazes, J. R. Rogers and N. M. Miskovsky, "Variational Formulation for the Equilibrium Condition of a Conducting Fluid in an Electric Field," Appl. Phys. A32, 55 (1983).

12. H. Gaubi, P. Sudraud, M. Tence and J. van der Walle, "Some New Results About in situ TEM Observations of the Emission Region in LMIS,' in Proceedings of the 29th Int. Field Emission Symposium ed by H. O. Andren and N. Norden (Almqvist and Wiksell International, Stockholm, 1982), p. 357.

13. A. Wagner, "The Hydrodynamics of Liquid Metal Ion Sources," Appl. Phys. Letts. 40, 440 (1982).

14. N. M. Miskovsky, P. H. Cutler and E. Kazes, "Derivation of the Condition for Onset of Instabilities of a Conducting Fluid Surface Under Electrostatic Stress: Application to Liquid Metal Ion Sources," to be published in J. Vac. Sci. and Technol., 1984.